

Simple Photocatalysis Model for Photoefficiency Enhancement via Controlled, Periodic Illumination

Santosh Upadhy and David F. Ollis*

Chemical Engineering Department, North Carolina State University, Raleigh, North Carolina 27695-7905

Received: August 30, 1996; In Final Form: November 28, 1996[®]

Under steady illumination, aqueous phase photocatalytic oxidation reactions using titanium dioxide characteristically exhibit low quantum yields, i.e., the incident light is used inefficiently in the process. Sczechowski, Koval, and Noble¹ reported substantially higher photoefficiencies (defined as reaction rate divided by incident photon rate) for TiO₂ while using controlled, periodic illumination instead of continuous illumination in a flow system. We propose a transient kinetic model which suggests that rapid consumption of preadsorbed reactant inventory by photoproduced holes (or by their oxidation product, OH radical, etc.) accounts for such high photoefficiencies with periodic illumination and that the characteristically slow adsorption of additional oxygen and/or electron transfer to oxygen is responsible for low quantum yields observed under steady illumination. A model simulation provides trends of photoefficiency with variation of the length of light and dark periods which resemble the observed photoefficiency trends, but fundamental comparisons await photoefficiency and individual rate constant measurements on the same photocatalysts.

1. Introduction

Sczechowski, Koval, and Noble¹ demonstrated a means of increasing the aqueous phase photoefficiency of formate ion oxidation by using a controlled, periodic illumination instead of continuous illumination of a TiO₂ catalyst suspension. They used a steady, open channel horizontal flow of a titania aqueous suspension under an aluminum cover with periodic slots cut to allow for recurring light exposures and intervening dark periods. They estimated that the top 1 mm depth of the 0.4 wt % titania suspension would absorb 99% of the light incident from above and that a particle at the topmost layer in the slurry absorbed approximately 250 photons in a 0.145 s exposure, whereas a particle at a depth 1 mm from the top absorbed only two to three photons in the same time interval. On average, about 50 photons per particle were absorbed through this 1 mm vertical depth during this exposure. Mass transfer of solutes (formate, oxygen) was shown to be a negligible resistance; thus, the observed kinetics were not influenced by the diffusional supply of oxygen or formate. A similar conclusion was reached earlier by Gerischer and Heller^{2b} for photocatalytic oxidation of organics under steady illumination.

The key experimental evidence in support of an enhancement effect of periodic illumination appears in Figure 1, parts a and b. The influence of varying the light period (Figure 1, part a) at a fixed dark period of 3 s indicates that a substantial increase in quantum efficiency is realized for illumination periods less than about one-third of a second (0.15 s was the shortest period examined). Similarly, the dark period is influential as well; increasing this variable to 1–3 s provided substantial enhancement again (Figure 1, part b). Particles subjected to repeated light and dark exposures provided the same measured quantum efficiencies as found with a single exposure; thus, the particle recovery appears complete at 1–3 s. Illumination times shorter than 0.15 s were not explored. The best exposure discovered was at 0.15 s light and 1.1 s dark time.

We present below a simple, transient model which attempts to rationalize this photoefficiency enhancement in terms of

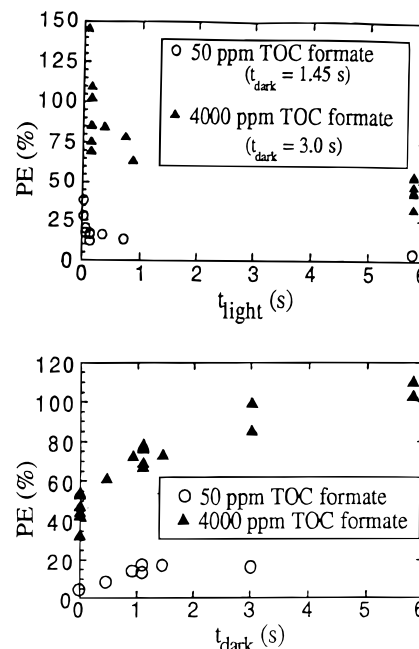


Figure 1. Photonic efficiency vs (a) illumination time, t_{light} , and (b) dark time, t_{dark} , for photocatalytic removal of formate in anatase(TiO₂) 0.4 wt % suspension.

fundamental steps. Aspects of the photocatalysis literature pertinent to parameter evaluation are summarized in Appendix 1.

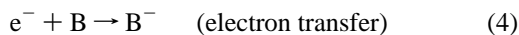
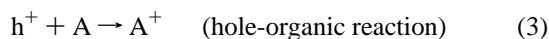
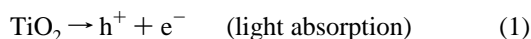
2. Model Formulation

We attempt to model the Sczechowski et al.¹ results in order to understand their observed phenomena of increased photoefficiency by use of alternate light and dark periods in place of continuous illumination. We consider the entire process to occur on a single TiO₂ particle as it moves through their open channel and experiences alternate light and dark periods. For the particle, the factors that affect quantum efficiency are light absorption, electron–hole recombination, electron transfer, organic oxidation, and, importantly, the depletion and replenish-

* Author to whom correspondence should be addressed.

[®] Abstract published in *Advance ACS Abstracts*, March 1, 1997.

ment of surface-adsorbed species. Thus, we have a simple kinetic scheme that involves the four familiar reactions below:



Our model considers A and B to be hydroxyl or formate ions and dioxygen, respectively, where both are adsorbed on the surface.

We adopt the following nomenclature:

k_g = light absorption rate constant

l = incident light intensity ($\text{s}^{-1} \text{cm}^{-3}$)

k_1 = oxidation reaction rate constant ($\text{s}^{-1} \text{cm}^{-3}$)

k_2 = electron transfer rate constant ($\text{s}^{-1} \text{cm}^{-3}$)

$k_2' = k_2 V$ ($\text{s}^{-1} \text{cm}^3$)

k_3 = dioxygen adsorption rate constant (s^{-1})

k_r = recombination rate constant ($\text{cm}^3 \text{s}^{-1}$)

Ω_A = surface fractional coverage by hydroxyl/formate ion

Ω_B = surface dioxygen coverage

n_A = number of surface sites for hydroxyl/formate (cm^{-2})

n_B = number of surface sites for dioxygen (cm^{-2})

(h^+) = hole concentration (cm^{-3})

(e^-) = electron concentration (cm^{-3})

V = TiO_2 volume (cm^3)

3. Equation Development

The instantaneous quantum yield of the TiO_2 -mediated oxidation of the organic can be defined as follows:

$$\begin{aligned} \phi &= \text{oxidation rate/photoexcitation rate} \\ &= k_1(\text{h}^+)\Omega_A/k_g l \end{aligned} \quad (5)$$

At steady state (ss), the illuminated solid forms holes which either react desirably at the surface or recombine, giving eq 6:

$$k_g l = k_1(\text{h}^+)\Omega_A + k_r(\text{h}^+)(\text{e}^-) \quad (6)$$

Combining (5) and (6) gives the predicted steady state quantum yield:

$$\phi_{ss} = k_1 n_A (\text{h}^+) \Omega_A / (k_1 n_A (\text{h}^+) \Omega_A + k_r (\text{h}^+) (\text{e}^-)) \quad (7)$$

or

$$\phi_{ss} = 1 / (1 + k_r (\text{e}^-) / k_1 n_A \Omega_A) \quad (8)$$

Thus, increasing surface coverage Ω_A of A and/or decreasing the electron concentration (e^-) would raise the quantum yield, with the ratio of rate constants for recombination and reaction dictating the extent of this change.

For their transient experiments, Sczechowski et al.¹ defined the quantum efficiency as the total moles of formate reacted per incident photon. Their measured photoefficiency is an integral of the instantaneous quantum yield over time. Consequently, an apt definition of their efficiency for our simple model would be a time-averaged value, ϕ :

$$\phi = \int k_1(\text{h}^+(t))\Omega_A(t) dt / \int k_g l dt \quad (9)$$

Here, a high photoefficiency would be expected for a high concentration of holes, (h^+), and a surface with 100% reactant coverage. Depletion of holes at any time by recombination would decrease this efficiency.

To generate a model reflective of the circumstances of the Sczechowski et al. studies,¹ we have to incorporate periodic illumination and calculate the resultant photoefficiency. For the particle experiencing periodic light and dark periods, we add the reaction occurring in the dark. Thus, the quantum yield for a periodic illumination experiment involving $t_{\text{tot}} = t_{\text{light}} + t_{\text{dark}}$ would be given by the following:

$$\phi_{\text{periodic}} = \int_{t_{\text{light}}+t_{\text{dark}}}^{\text{light}} k_1 n_A (\text{h}^+(t)) \Omega_A(t) dt / \int_{t_{\text{light}}+t_{\text{dark}}}^{\text{light}} k_g l dt \quad (10)$$

The quantum yield for a similar but continuous light exposure time experiment will be a steady state (ss) expression:

$$\phi_{\text{continuous}} = \int_{t_{\text{light}}}^{\text{light}} k_1 n_A (\text{h}^+)_{ss} \Omega_{A_{ss}} dt / \int_{t_{\text{light}}}^{\text{light}} k_g l dt \quad (11)$$

Periodic illumination drives transient levels of every reactant and intermediate in the system, and transient concentration balances are required for each reactive species.

Previous Transient Models. Nosaka and Fox⁵ modeled hole and electron transients, but did not include a concentration dependence for either the methyl viologen being reduced or the oxidizable adsorbed species. Rate constants were evaluated, but no simulation presented.

Mills and Williams²⁹ proposed a steady state model for CdS photoreduction of methyl orange in the presence of oxygen, with EDTA used as a hole scavenger. The Mills and Williams model involved only continuous, and not transient, operation.

Neither model suggested inclusion of transients in the inventory of surface reactant species. The model developed below includes this feature, which is a key to our proposed interpretation of the quantum efficiency enhancement obtained with periodic illumination.

Present Model. The hole and electron transient balances yield (12) and (13):

$$d(\text{h}^+)/dt = k_g l - k_r(\text{h}^+)(\text{e}^-) - k_1(\text{h}^+)n_A\Omega_A \quad (12)$$

$$d(\text{e}^-)/dt = k_g l - k_r(\text{h}^+)(\text{e}^-) - k_2(\text{e}^-)n_B\Omega_B \quad (13)$$

The central assumption here is that either (i) oxygen replenishment by adsorption from the solution or (ii) electron transfer to (adsorbed) oxygen is the slow step during steady illumination. Thus, use of periodic illumination and darkness provides the dark time intervals required (i) to allow redevelopment of appreciable surface oxygen coverage or (ii) to allow completion of electron discharge to adsorbed oxygen (and completion of follow-on reactions).

We consider first slow adsorption by B, dioxygen, which is the presumed electron acceptor. For this slow adsorption, we

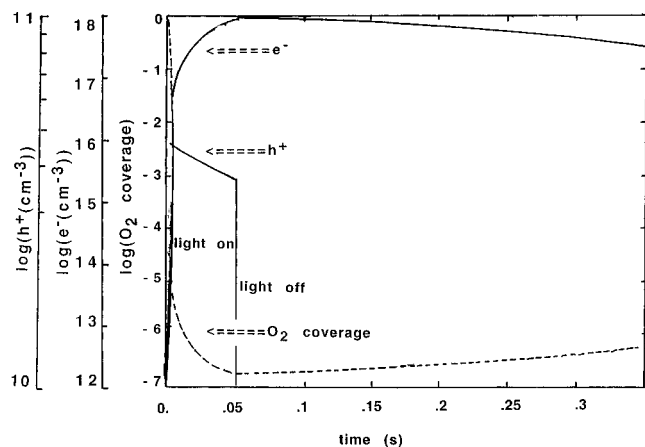


Figure 2. Model profiles calculated for hole, dioxygen, and electron concentrations vs time in a single light and dark cycle. $t_{\text{light}} = 50$ ms. $t_{\text{dark}} = 1.45$ s.

assume hydroxyl (or formate) coverage to be constant (i.e., equilibrated at all times) and consider only the replenishment dynamics of dioxygen. Adding the adsorbed oxygen balance gives knowledge of all variables which affect the photoefficiency:

$$d\Omega_B/dt = k_3(1 - \Omega_B) - k_2(e^-)n_B\Omega_B \quad (14a)$$

where the first and second terms respectively represent oxygen replenishment by adsorption and adsorbed oxygen reaction via electron charge transfer. For simplicity, oxygen desorption is not considered.

In an alternate, second case, the electron transfer to (adsorbed) oxygen is slow, and we would take dioxygen coverage to be ample and constant. The oxygen coverage, Ω_B , would be determined from 14b:

$$d\Omega_B/dt = 0 = k_3(1 - \Omega_B) - k_3n_B\Omega_B \quad (14b)$$

where the two right-hand terms represent respectively oxygen adsorption and desorption.

We solve the first case as discussed below and comment on the predicted results and their relation to the literature.

4. Model Solution

We adopted the MATLAB ODE 15s solver for the stiff set of differential equations (12–14), since we expected large time gradients in the transient responses of these system variables. The initial conditions for the holes and electrons were assumed to be zero (arbitrarily small) before the TiO_2 surface was illuminated. The initial coverage of hydroxide ion was assumed to be unity.

5. Results and Discussion

Adsorption of the electron acceptor is assumed to be slower than organic or hydroxide adsorption. This circumstance may apply more often than the converse. In this case, electron donor adsorption is assumed to be equilibrated at all times.

Hole, Electron, and Dioxygen Concentrations vs Time. Figure 2 illustrates a typical calculation for the case of an illumination period of 0.05 s, a dark period of 1.45 s, and an adsorption rate constant of intermediate magnitude, 30 s^{-1} . The corresponding time profiles calculated for holes, electrons, and adsorbed dioxygen indicate the following: (1) With commencement of illumination, the adsorbed oxygen reacts rapidly with the photoproduced electrons and the former falls to a very low value within 0.05 s, leading to a subsequent accumulation of

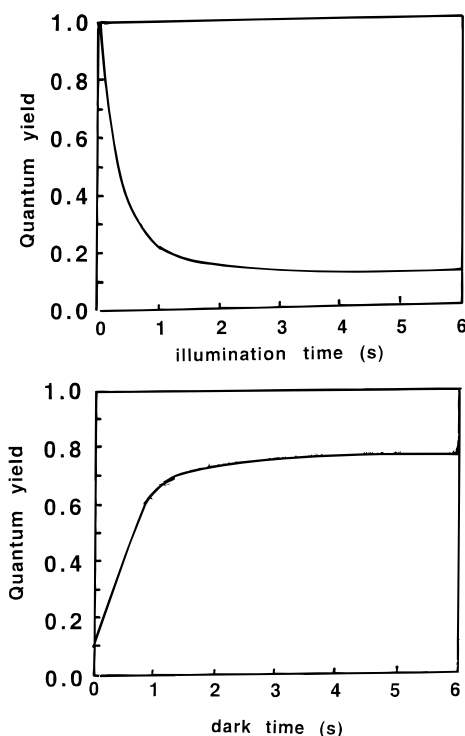


Figure 3. Model calculations of quantum yield vs (a) light period duration, t_{light} ($t_{\text{dark}} = 1.45$ s, $I = 2.44 \times 10^{19} \text{ cm}^{-3} \text{ s}^{-1}$), and (b) dark period duration, t_{dark} ($t_{\text{light}} = 0.15$ s, $I = 2.44 \times 10^{19} \text{ cm}^{-3} \text{ s}^{-1}$).

electrons. The holes concentration rises almost immediately to a finite low value and declines slowly over the first 0.05 s due to the increasing recombination velocity caused by rising electron levels. (2) When illumination ceases at 0.05 s, the relatively high electron concentration quickly titrates all holes and concentration of the latter drops precipitously, effectively stopping the desired oxidation reaction, despite a continued adequate coverage by the electron donor. The exhausted dioxygen coverage recovers only slowly, and consequently the accumulated electrons are only slowly discharged. The dark period is thus devoted almost exclusively to regeneration of a surface repopulated with sufficient dioxygen to receive and remove further electrons produced in the next illumination cycle.

Photoefficiency Variation with Light and Dark Exposure Times. With the kinetic parameters fixed at the base case values in Appendix 2, we calculate the predicted variation in photoefficiency (PE) as a function of light and dark illumination times, since Sczechowski et al.¹ reported their efficiency variation in these terms (Figure 1 parts a and b). Our calculated results appear in Figure 3, parts a and b. Absolute values aside, we are encouraged by the general trends: (i) For variation of illumination time, the PE rises as t_{light} decreases and is most pronounced at times less than 0.3 s, in agreement with Figure 1, part a. (ii) Similarly, a slow readsorption time for dioxygen results in an improved PE with increasing dark adsorption time, Figure 3, part b, consistent with the experimental trends reported for the formate concentrations in Figure 1, part b.

Model Sensitivity Analysis to Readsorption Time. As we do not have a well-defined knowledge of the model parameters, but only reasonable average values or estimates, this level of agreement for an early, very simple model is encouraging.

We now illustrate the model sensitivity to the presumed smallest rate constant k_3 , that for dioxygen adsorption.

Figure 4, parts a and b, presents the calculated time variation of the adsorbed dioxygen concentration for values of the adsorption constant k_3 equal to 10 and 0.1 times the base case value of 30 s^{-1} . Under illumination, the adsorbed O_2 coverage

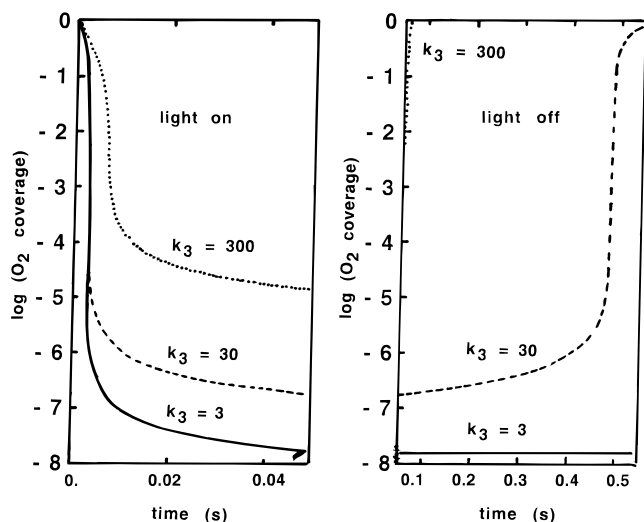


Figure 4. Calculated dioxygen coverage vs adsorption rate constant k_3 during light (A) and dark (B) periods.

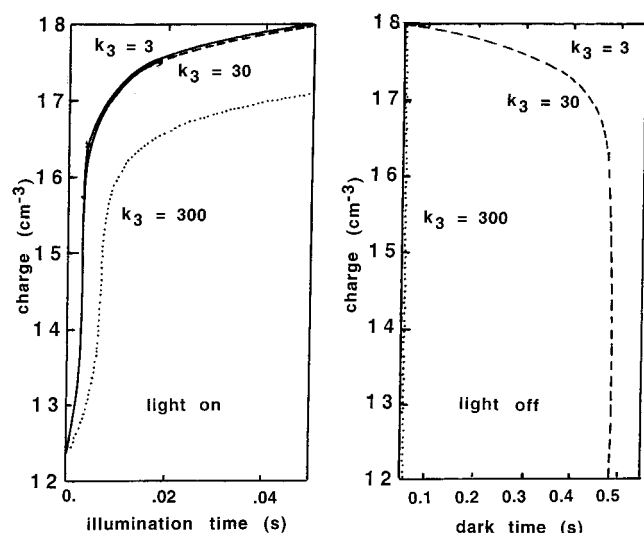


Figure 5. Model calculation of net charge concentration, (net) = (e^-) - (h^+), vs light (left) and dark (right) periods for various readsorption rate constant (k_3) values.

falls rapidly for $k_3 = 30$ or 3 s^{-1} , but more slowly at $k_3 = 300 \text{ s}^{-1}$, and to a lesser minimum value at 0.05 s. In the dark period, the low value of $k_3 = 3 \text{ s}^{-1}$ produces little new adsorption during 1.45 s because a long recovery time of ca. 30 s would be expected. Similarly, for $k_3 = 300 \text{ s}^{-1}$, a very rapid repopulation of the surface by O₂ occurs, and the required dark exposure time for this circumstance is very small.

The net charge of a particle is measurable and is calculated from the model (Figure 5, parts a and b). The predicted excess of electrons over holes, under all illumination and dark circumstances, indicates that the particle will be negatively charged. With illumination (Figure 5, part a), the smaller adsorption rate constant values give nearly identical particle-charging curves, whereas $k_3 = 300 \text{ s}^{-1}$ provides the expected 10-fold reduction in the nearly steady state maximum charge achieved. The dark period is most sensitive to the adsorption constant: $k_3 = 300 \text{ s}^{-1}$ gives a nearly immediate discharge of electrons, due to a combination of a 10-fold smaller starting electron concentration at the dark period beginning and a 10-fold greater rate constant. With the base case, discharge is complete in 0.5 s, and at k_3 equal to one-tenth the base case value, no noticeable electron discharge is predicted within this time interval.

The net negative charge arises because electron discharge is slow relative to hole reactions. It may be slow due to slow adsorption of additional oxygen on the surface to remove excess electrons (model calculations here) or slow due to charge transfer from (trapped) electrons to adsorbed oxygen as argued by Gerischer and Heller^{2a,b} among others. The model simulation of Figure 5 is consistent with the observations of Chang, Heller, and Gerischer^{2c} that, in 1.6 M aqueous methanol, titania slurry particles can retain negative charge for relatively long periods, e.g., 1 min, even in oxygen-saturated solutions.

Periodic illumination increases the photoefficiency of photocatalyzed oxidation. So does metallization of titania under steady illumination, e.g., ref 2c, and these two enhancements appear to be related. The Szechowski et al.¹ results of Figure 1, parts a and b, indicate enhancement of the oxidation of the carboxylate, formate, by factors of 2- to 10-fold vs the smallest values shown at long illumination time (5 s, which is probably near the steady state value). Similarly, addition of 0.01–2 wt % Pd to titania increased the quantum yield of a second carboxylate oxidation, that of 2,2-dichloropropionate (DCP), by 3- to 7-fold at 0.01 M DCP. Both results are consistent with operation under conditions which favor electron transfer and/or oxygen adsorption vs those for steady illumination of native TiO₂.

A second model possibility is slow electron transfer to adsorbed oxygen. This could be modeled using (14b) along with the previous equations for the transient hole and electron balances. It is evident that a sufficiently slow electron transfer rate constant would produce similar trends in the calculated photoefficiencies, and the present example is therefore illustrative, but not definitive, in part due to uncertainties in the relative slowness of adsorption vs electron transfer.

The nature of the oxygen reduction dilemma is illustrated by an example for iron, for which Bockris and Khan²⁹ indicate that the rate-determining step on bare iron is $\text{O}_2 + e^- \rightarrow \text{O}_2^-$, while the slow step on passive iron (hydrated iron oxide surface) appears to be chemisorption (Sepa et al.²⁸): $\text{O}_2 \rightarrow \text{O}_{2\text{ads}}$, as we assumed for these calculations.

The present model is speculative, but the agreement of the photoefficiency trends in Figure 1 (experimental) and Figure 3 (model) with periodic exposure times, light and dark, suggests that better models which are more accurate and more detailed, built along similar lines, may provide a fruitful path to understanding and improving the aqueous phase photoefficiencies. This area needs substantial further attention if photocatalytic water treatment is to be understood well and is to compete with other advanced oxidation processes.

Acknowledgment. During this work, S. Upadhyaya was supported by a Hoechst-Celanese Kenan Fellowship for Environmental Science and Technology.

Appendix 1

This appendix summarizes the evidence for the following items which support the present model: (1) Intraparticle excitation, transport, and trapping of holes and electrons are rapid compared to the approximately 1 s relaxation time evident in Figure 1, parts a and b. (2) Electron transfer to dioxygen is widely presumed to be a slow step in aqueous phase photocatalysis, but this claim is ambiguous: if dioxygen adsorption must precede charge transfer, then adsorption or charge transfer are both possible slow steps. Calculations for slow adsorption appear in Figures 2–4; the second case would give similar results with an appropriate small rate constant.

Electron and Hole Dynamics in TiO₂. Gratzel and Frank³ examined (i) charge carrier diffusion from the particle interior, (ii) encounter-complex formation, and (iii) interfacial electron transfer, finding the first to be very rapid (10^{-12} s) and the second and third to have relaxation times of the order of nanoseconds (10^{-9} s). Their model led to a diffusion-limited supply of electron acceptor from bulk solution; however, no allowance was made for acceptor adsorption. Rothenberger et al.⁴ determined average hole and electron lifetimes in colloidal TiO₂ in water, reporting a second-order recombination rate constant of 10^7 s⁻¹ and a first-order hole-trapping rate constant of 4×10^6 s⁻¹. Electron transport and trapping at the surface were very rapid by comparison.

Nosaka and Fox⁵ used pulsed laser experiments with methyl viologen and determined rate constants k_e , k_h , and k_r for first-order electron transfer and hole transfer and for second-order recombination respectively to be $k_e > 10^{10}$ s⁻¹, $k_h > 10^{10}$ s⁻¹, and $k_r > 10^{-6}$ cm⁻³ s⁻¹.

Colombo et al.⁶ used diffuse reflectance spectroscopy with femtosecond resolution to show that titania nanoclusters (2 nm) and Degussa P-25 powders (30 nm primary particle diameter) exhibited similar behavior: with rapid electron trapping, second-order recombination of surface-trapped electrons, and longer lived interstitially trapped electrons, experiments in water were not carried out.

Gerischer and Heller² analyzed electron transfer to dioxygen during the photocatalyzed destruction of organics.

Charge Carrier Transfer to the Surface. Bahneman et al.⁷ reviewed the charge transit literature for migration to the semiconductor surface and concluded this to be extremely fast. Recently, Hoffman et al.⁸ summarized characteristic times for photocatalysis, concluding from their own laser flash photolysis measurements that charge trapping occurs in 100 ps to 10 ns, charge carrier recombination takes place in periods of 10–100 ns, and interfacial charge transfer is the slowest, especially for electron transfer (milliseconds). Our model assumes charge transit and trapping to be instantaneous within the time domain modeled 10^{-3} to 3 s.

Recombination Dynamics. Duonghong et al.⁹ considered reaction between conduction band electrons and methylviologen (MV²⁺) to be unlikely and inferred an electron lifetime to be at least of the order of milliseconds. Rothenberger, et al.⁴ calculated electron-hole recombination rate constants of 10^7 s⁻¹. Henglein¹⁰ reported an upper lifetime limit of 30 ns for holes with respect to recombination on 30–100 nm TiO₂ particles.

Colombo et al.^{6b} found 2 nm TiO₂ particles to possess a bulk reaction rate constant of 4.3×10^{10} s⁻¹ for recombination of trapped electrons.

In our model, we assume an approximate consensus value of electron-hole lifetimes of 100 ns.

Interfacial Electron Transfer. Brown et al.¹¹ characterized the interfacial kinetics of electron transfer to acceptors such as MV²⁺ by an average rate constant for the heterogeneous system of $k_x = 180$ s⁻¹ and 10 s⁻¹ for 18 and 6 nm particles, respectively.

Kasinski et al.¹² conducted surface-restricted transient grating studies of aqueous TiO₂ and suggested a hydroxide ion to be the initial hole acceptor. With doping levels of 10^{19} cm⁻³ and pH = 13.5, two time constants of 460 ps and 4.8 ns were attributed respectively to reduction of holes generated within the space charge region and to diffusion of bulk electron-hole pairs into the space charge layer where recombination and interfacial electron transfer rates were assumed high.

Martin et al.¹³ studied postexcitation charge carrier dynamics of P-25 and determined an interfacial electron transfer rate

constant of 65 s⁻¹ using time-resolved microwave conductivity measurements.

In our model, we will assume the primary interfacial electron reaction to be transfer to molecular oxygen, following Gerischer and Heller.²

Electron Transfer to Oxygen. Brown and Darwent¹⁴ examined methyl orange oxidation and simultaneous oxygen photoreduction on TiO₂ colloids and calculated the dimensionless ratio of the recombination to hole reaction rate constants to be 450. The rate constant for dioxygen reduction by electrons, calculated to be $k_o = 3.3 \times 10^8$ dm³ mol⁻¹ s⁻¹ at pH 11.2, gives an apparent first-order rate constant, $k_o(\text{O}_2) = 6 \times 10^4$ s⁻¹, for an oxygen-equilibrated solution.

Brown et al.¹⁵ later measured a rate of electron transfer to oxygen, fitted to the following expression:

$$\text{rate} = (5.5 \times 10^3)(\text{O}_2)(e^-)/(h^+)^{0.42} (\text{mol dm}^{-3})^{-0.58} \text{ s}^{-1}$$

Using their expression, we calculate an electron transfer rate constant of 766 s⁻¹, assuming a pH 7 for the oxygen-equilibrated solution (similar to conditions of Sczechowski et al.¹).

Hole Transfer Reactions. Moser and Gratzel¹⁶ investigated reactions of valence band holes with halide ions following laser excitation of aqueous TiO₂ sols and found hole transfer to take place within 10 ns. For the aqueous formate solutions of Sczechowski et al.,¹⁻³ we will assume in our model that only an adsorbed hydroxide or formate ion is involved in the primary, rapid reaction with holes.

Hydroxyl Ion Oxidation by Holes. Salvador¹⁷ suggested that the primary charge transfer steps were the holes reacting with OH⁻ ions and electrons with Ti⁴⁺ ions. Lawless et al.¹⁸ used pulse radiolysis to study the role of OH radicals in photocatalysis. An adsorbed hydroxyl radical was shown to have very strong oxidizing abilities. The authors argued that a trapped hole and surface bound OH radical were indistinguishable in photocatalysis, since the free hole would react with a water molecule and create an adsorbed OH radical. The results were consistent with the adsorbed hydroxyls becoming the major oxidants, and the desorption of OH radicals into the solution was viewed as unlikely. Kormann et al.¹⁹ studied the photocatalytic degradation of chloroform in aqueous TiO₂ suspensions. Assuming holes to have longer lifetimes than electrons, the authors argued that holes were scavenged by the hydroxylated TiO₂ surface, forming hydroxyl radicals. The rate-limiting reaction of the surface hydroxyl groups with the adsorbed chloroform was incorporated in their proposed reaction mechanism.

Necessary Preadsorption. Grabner and Quint²⁰ used laser pulses of various total number of photons to study methyl viologen reduction and oxidation of halide ions in aqueous TiO₂ suspensions. The authors obtained transient absorbance signals for the product formed (MV¹⁺ or Cl₂⁻) which were proportional to the original amount of reactant adsorbed (MV²⁺ or Cl⁻). They suggest that depletion of surface-adsorbed reactants at higher photon doses was a plausible cause for the observed decrease in reaction rate with increasing photon dose. Calculating similar orders of magnitude for the initial adsorbed reactant and the incident photon dose, the authors noted the surface adsorption rate could not be ignored, since holes produced from the incident photons would react with the adsorbed reactant and deplete the reactant surface coverage if the readsorption rate was not sufficiently fast. Using variable photon doses and plotting the reciprocal of quantum yield vs reciprocal of the initial adsorbed methyl viologen concentration C_{ads} , the authors obtained a straight line, yielding a corresponding empirical formula for the quantum yield ϕ :

$$\phi = k_1 C_{\text{ads}} / (k_1 C_{\text{ads}} + k_2)$$

The expression indicates a competition between the reaction of adsorbed species and another pseudo-first-order reaction for the same charge carrier. The three possibilities suggested for the latter were (i) carrier trapping at sites causing reduced charge transfer to reactants, (ii) reaction with coadsorbants, and (iii) electron-hole recombination.

Draper and Fox²¹ suggested the possibility of direct hole transfer as well as OH radical mediated oxidation as the primary photooxidation step for organic species. Subsequently, Fox et al.³⁰ reasoned that preadsorption of the carrier-trapping species before absorption of light was essential for the hole trapping to be kinetically favorable vs electron-hole recombination. Our model will assume that charge transfer occurs only between adsorbed species (hydroxyl/formate and oxygen) and charge carriers (holes and electrons, respectively).

Oxygen Surface Adsorption. Okamoto et al.²² studied phenol oxidation in aqueous suspensions of TiO₂, observed a Langmuirian reaction dependence on dissolved oxygen, and claimed that adsorbed oxygen prevented recombination of electron-hole pairs though trapping electrons to form superoxide ions. Later,²³ they reported an oxygen adsorption constant to be 270.6 M⁻¹.

Kormann et al.¹⁹ described oxygen influence on chloroform with titania suspensions to fit a surface-binding constant of 13 × 10⁴ M⁻¹.

Experimental observation of Gratzel and Frank³ suggested a small electron transfer rate constant to adsorbed oxygen, i.e., 3 s⁻¹. Higher theoretical values of 10⁷ s⁻¹ were estimated by Gerischer and Heller,² but these authors noted that rates could be reduced to the order of 3 s⁻¹ either by weak overlap between the adsorbed oxygen orbitals and the electrons or by electron reaction from surface traps. They also suggested that the photoefficiency of the TiO₂-photoassisted oxidation of organic compounds in water was limited by the kinetics of the oxygen reduction.

Gerischer²⁴ calculated a minimum rate constant value to be 10 cm s⁻¹ for electron transfer to oxygen for a particle of radius 1 μm, incorporating the electrostatic repulsion that favors movement of excess charges closer to the particle surface. Gerischer²⁵ next estimated a theoretical, second rate constant value for the reduction of oxygen to be 4.6 × 10⁻²⁰ cm⁴ s⁻¹ or with air-equilibrated oxygen present in solution, $k_{\text{red}}\text{CO}_2 < 8 \times 10^{-3} \text{ cm s}^{-1}$. Our proposed model assumes interfacial electron transfer to adsorbed oxygen to occur on the order of hundredths of seconds.

Surface Site Densities. Lawless et al.¹⁸ cite a value of 5–15 OH⁻ groups per square nanometer for TiO₂ surface coverage. Munuera et al.²⁶ reported coverages of water on the TiO₂ surface to be 5 × 10¹⁴ cm⁻² molecules along with 3 × 10¹⁴ cm⁻² acidic OH groups and 2 × 10¹⁴ basic OH groups. We assume 5 × 10¹⁴ cm⁻² total value of surface hydroxyl groups in our model. Gerischer²⁴ suggests that the oxygen concentration at the particle surface is constant, provided the solution remains equilibrated with oxygen. In our model, we assume that, at pH 7, the formate and hydroxyl ion concentrations are constant and that the adsorption of dioxygen is slow, and thus kinetically important during periodic illumination of interest.

Appendix 2. Base Case Parameter Values

1. Photon absorption rate per particle: Sczechowski et al.¹ calculated an average of 50 photons per particle absorbed in 145 ms:

$$k_g I (\text{cm}^{-3} \text{s}^{-1}) = 50 / [(145 \times 10^{-3}) V] = 2.44 \times 10^{19} \text{ cm}^{-3} \text{s}^{-1}$$

where V = volume of illuminated particle.

2. Recombination lifetimes of the order of 10–100 ns have been reported. Assume recombination rate constant to be 10⁻⁷ s⁻¹:

$$k_r (\text{cm}^3/\text{s}) = 10^{-7} V$$

3. Electron transfer to oxygen of the order of milliseconds has been observed. Assume the electron transfer rate constant to be 10³ s⁻¹:

$$k_2 (\text{cm}^2 \text{s}^{-1}) = 10^3 V a \beta$$

where catalyst surface area a (cm² g⁻¹) = 50 × 10⁴ and catalyst density β (g cm⁻³) = 3.8.

4. Hole transfer is assumed to have a rate constant of 4 × 10⁴ s⁻¹ on the basis of the ratio of recombination to reaction being 450.¹⁷

$$k_1 (\text{cm}^2 \text{s}^{-1}) = (4 \times 10^4) V a \beta$$

5. We assume the density of all adsorption sites to be 5 × 10¹⁴ cm⁻².

$$n_A (\text{cm}^{-2}) = n_B (\text{cm}^{-2}) = 5 \times 10^{14}$$

6. We have no data for O₂ adsorption rate. We assume $k_3 = 30 \text{ s}^{-1}$. (This k_3 value is consistent with apparent charge transfer kinetics cited in Appendix 1, which must include both adsorption and charge transfer fundamental steps), e.g., from 10 to 180 s⁻¹ (Martin et al.¹¹), 65 s⁻¹ (Martin et al.¹³), and 766 s⁻¹ (Brown et al.¹⁸).

References and Notes

- (1) (a) Sczechowski, J. G.; Koval, C. A.; Noble, R. A. *J. Photochem. Photobiol., A* **1993**, *74*, 273. (b) Sczechowski, J. G.; Bader, K. E.; Koval, C. A.; Noble, R. D. *J. Photochem. Photobiol., A* submitted for publication. (c) Sczechowski, J. G.; Koval, C. A.; Noble, R. D. In *Photocatalytic Purification and Treatment of Water and Air*; Ollis, D. F., Al-Ekabi, H., Eds.; Elsevier: Amsterdam, 1993; pp 645–650.
- (2) (a) Gerischer, H.; Heller, A. *J. Phys. Chem.* **1991**, *95*, 5261. (b) Gerischer, H.; Heller, A. *J. Electrochem. Soc.* **1992**, *139*, 113. (c) Chang, C.-M.; Heller, A.; Gerischer, H. *J. Am. Chem. Soc.* **1992**, *114*, 5230.
- (3) Gratzel, M.; Frank, A. *J. Phys. Chem.* **1982**, *86*, 2964.
- (4) Rothenberger, G.; Moser, J.; Gratzel, M.; Serpone, N.; Sharma, D. K. *J. Am. Chem. Soc.* **1985**, *107*, 8054.
- (5) Nosaka, Y.; Fox, M. A. *J. Phys. Chem.* **1988**, *92*, 1893.
- (6) (a) Colombo, D. P., Jr.; Roussel, K. A.; Sach, J.; Skinner, D. E.; Cavaleri, J. J.; Brown, R. M. *Chem. Phys. Lett.* **1995**, *232*, 207. (b) Colombo, D. P., Jr.; Bowman, R. M. *J. Phys. Chem.* **1995**, *99*, 11752.
- (7) Bahneman, D. W. In *Photochemical Conversion and Storage of Solar Energy*; Pelizzetti, E., Schiavello, M., Eds.; Kluwer: The Netherlands, 1991; pp 251–276.
- (8) Hoffman, M. R.; Martin, S. T.; Choi, W.; Bahnemann, D. W. *Chem. Rev.* **1995**, *95*, 69–96.
- (9) Duonghong, D.; Ramsden, J.; Gratzel, M. *J. Am. Chem. Soc.* **1982**, *104*, 2977.
- (10) Henglein, Ber. *Bunsen-Ges. Phys. Chem.* **1982**, *86*, 241.
- (11) Brown, G. T.; Darwent, J. R.; Fletcher, P. D. I. *J. Am. Chem. Soc.* **1985**, *107*, 6446.
- (12) Kasinski, J. J.; Gomez-Jahn, L. A.; Faran, K. J.; Gracewski, S. M.; Miller, R. J. D. *J. Chem. Phys.* **1989**, *90*, 1253.
- (13) Martin, S. T.; Herrmann, H.; Choi, W.; Hoffman, M. R. *J. Chem. Soc., Faraday Trans.* **1994**, *90*, 3315.
- (14) Brown, G. T.; Darwent, J. R. *J. Phys. Chem.* **1984**, *88*, 4955.
- (15) Brown, G. T.; Darwent, J. R. *J. Chem. Soc., Faraday Trans.* **1984**, *80*, 1631.
- (16) Moser, J.; Gratzel, M. *Helv. Chim. Acta* **1982**, *65*, 1436.
- (17) Salvador, P. *J. Electrochem. Soc.* **1981**, *128*, 1985.
- (18) Lawless, D.; Serpone, N.; Meisel, D. *J. Phys. Chem.* **1991**, *95*, 5166.

- (19) Kormann, C.; Bahnemann, D. W.; Hoffmann, M. R. *Environ. Sci. Technol.* **1991**, 25, 494.
- (20) Grabner, G.; Quint, R. M. *Langmuir* **1991**, 7, 1091.
- (21) Draper, R. B.; Fox, M. A. *Langmuir* **1990**, 6, 1396.
- (22) Okamoto, K.; Yamamoto, Y.; Tanaka, H.; Tanake, M.; Itaya, A. *Bull. Chem. Soc. Jpn.* **1985**, 58, 2023.
- (23) Okamoto, K.; Yamamoto, Y.; Tanaka, H.; Tanake, M.; Itaya, A. *Bull. Chem. Soc. Jpn.* **1985**, 58, 2023.
- (24) Gerischer, H. *Electrochim. Acta* **1993**, 38, 3.
- (25) Gerischer, H. In *Photocatalytic Purification and Treatment of Water and Air*; Ollis, D. F., Al-Ekabi, H., Eds.; Elsevier: Amsterdam, 1993; pp 1–17.
- (26) Munuera, G.; Rives-Arnau, V.; Saucedo, A. *J. Chem. Soc., Faraday Trans.* **1979**, 75, 736.
- (27) Bockris, J. O'M.; Khan S. U. M. *Surface Electrochemistry*; Plenum Press: New York, 1993; p 334.
- (28) Sepa, D. G.; Voinovic, M. V.; Vracar, L. M. *Electrochim. Acta* **1986**, 31, 1105.
- (29) Mills, A.; Williams, G. *J. Chem. Soc., Faraday Trans.* **1987**, 83, 2647.
- (30) Fox, M. A.; Draper, R. B.; Duloy, M.; O'Shea, K. *Photochemical Conversion and Storage of Solar Energy*; Pelizzetti, E., Schiavello, M., Eds.; Kluwer Academic Publishers: Amsterdam, 1991; p 323.